Geophysical Research Letters

RESEARCH LETTER
10.1029/2018GL078568

Key Points:
- Deep water oxygenation changes in the South China Sea since the last glacial period have mirrored those in Pacific deep water
- The strengthened North Pacific Intermediate Water did not influence South China Sea deep water during cold stadials of the last deglacial period
- A strengthened intermediate-depth meridional overturning occurred in the western Pacific Ocean during cold stadials of the last deglacial period

Supporting Information:
- Supporting Information S1
- Data Set S1

Correspondence to:
L. Zhong,
zhonglf9@mail.sysu.edu.cn

Citation:
Li, G., Rashid, H., Zhong, L., Xu, X., Yan, W., & Chen, Z. (2018). Changes in deep water oxygenation of the South China Sea since the last glacial period. *Geophysical Research Letters*, *45*, 9058–9066. https://doi.org/10.1029/2018GL078568

Received 29 APR 2018
Accepted 14 AUG 2018
Accepted article online 24 AUG 2018
Published online 5 SEP 2018

Changes in Deep Water Oxygenation of the South China Sea Since the Last Glacial Period

Gang Li[1], Harunur Rashid[2,3], Lifeng Zhong[4], Xing Xu[5], Wen Yan[1,6], and Zhong Chen[1]

[1]Key Laboratory of Ocean and Marginal Sea Geology, South China Sea Institute of Oceanology, Chinese Academy of Sciences, Guangzhou, China, [2]Earth and Environmental Sciences, Memorial University of Newfoundland, St. John's, Canada, [3]Hadal Science and Technology Research Center, Shanghai Ocean University, Shanghai, China, [4]School of Marine Sciences, Sun Yat-Sen University, Guangzhou, China, [5]Guangzhou Marine Geological Survey, Ministry of Land and Resources, Guangzhou, China, [6]School of Marine Sciences, University of Chinese Academy of Sciences, Beijing, China

Abstract The Pacific meridional overturning circulation is thought to have a significant influence on global climate. However, the extent to which intermediate and deep circulations have changed in the Pacific Ocean since the Last Glacial Maximum (LGM) is not well known. At present, the South China Sea Deep Water (SCSDW) is fed by the upper Pacific Deep Water. Here we present new benthic foraminiferal $\delta^{13}C$ and redox-sensitive elemental data from a sediment core retrieved from the southern deep SCS to reconstruct the oxygenation history of the SCSDW since the LGM. Oxygenation records from the deep SCS and intermediate and deep waters in the Pacific Ocean demonstrate that the SCSDW deeper than 1,600 m has been sourced by the Pacific Deep Water since the LGM. Our data suggest that the well-ventilated North Pacific Intermediate Water would not have influenced the SCSDW during cold stadials of the last deglacial period.

Plain Language Summary The global ocean circulation has an important role in influencing the climate. Large-scale change in global ocean circulation has occurred since the last glacial period. In comparison to the Atlantic Ocean, oxygenation data from the intermediate and deep waters of the Pacific Ocean are relatively poor. At present, the South China Sea Deep Water (SCSDW) is mainly fed by the Pacific Deep Water. In this contribution, we present new carbon isotope data on bottom-water-living protists and abundance of redox-sensitive elements that highlight the availability of oxygen from a sediment core in the southern deep SCS. The data allow reconstruction of the oxygenation history of the SCSDW for the past 30,000 years. Our data are compared with other published oxygenation records from intermediate and deep waters in the Pacific Ocean. The combined oxygenation records demonstrate that the SCSDW would have been sourced by the Pacific Deep Water since the Last Glacial Maximum (21,000 years before present). The oxygenation records in the deep SCS appear to support the general circulation model results and paleo-proxy data in the North Pacific, which suggest that a strengthened meridional overturning mainly occurred within intermediate waters during cold stadials of the last deglacial period.

1. Introduction

The atmospheric CO_2 concentration during the Last Glacial Maximum (LGM) was ~80 ppm lower than that of the Holocene (Monnin et al., 2001). Changes in the global ocean circulation are regarded as significant contributors to the atmospheric CO_2 rise during the deglacial period (Köhler et al., 2005; Sigman & Boyle, 2000). The North Pacific is a terminus in the modern routing of deep water circulation, and the old Pacific Deep Water (PDW) is one of the most important CO_2 reservoirs (Broecker et al., 2004). Hence, the reconstruction of the Pacific meridional overturning circulation is essential for understanding the role of ocean in modifying the atmospheric CO_2 concentration.

At present, no deep water is formed in modern subarctic Pacific as a permanent halocline leads to a strong stratification of the surface ocean (Warren, 1983). The deep North Pacific is slowly replenished by the North Atlantic Deep Water and the Antarctic Bottom Water from the Southern Ocean (Talley, 2013). Studies have pointed out fundamental changes in the Pacific meridional overturning circulation during the last deglacial stadials (Costa et al., 2018; Mikolajewicz et al., 1997; Okazaki et al., 2010; Rae et al., 2014). A few modeling studies suggested that the breakdown of the permanent halocline in the subarctic Pacific created well-

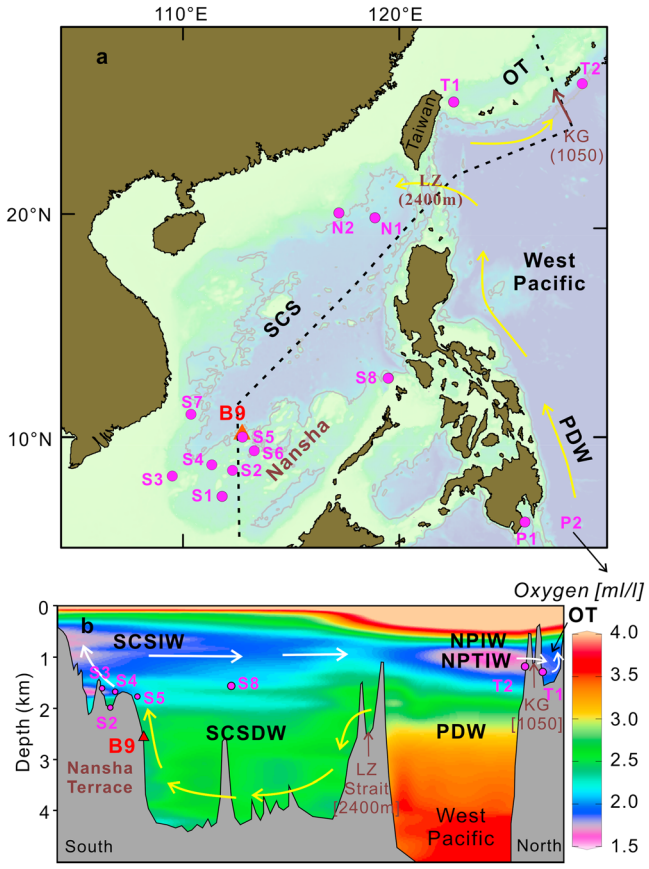

Figure 1. (a) Bathymetry of the western Pacific Ocean. The core B9 is labeled by a red triangle (this study). Solid circles correspond to the location of reference cores/boreholes VM35-6 (S1), GIK17961 (S2), MD97-2151 (S3), MD05-2896 (S4), NS93-5 (S5), ODP1143 (S6), NS90-103 (S7), MD97-2142 (S8), GIK17925 (N1), ODP1144 (N2), ODP1202B (T1), GH08-2004 (T2), MD98-2181 (P1), and MD01-2386 (P2). (b) The meridional bathymetric profile (along the dashed line in Figure 1) of dissolved oxygen content from the South China Sea to the Okinawa Trough was generated by Ocean Data View (Schlitzer, 2002) based on World Ocean Atlas (Garcia et al., 2014). Arrows mark the route of the PDW and the schematic deep circulation in the SCS and OT. The greatest depths of Luzon Strait (LZ) and Kerama Gap (KG) are labeled. NPIW = North Pacific Intermediate Water; NPTIW = North Pacific Tropical Intermediate Water; PDW = Pacific Deep Water; SCSDW = South China Sea Deep Water; SCSIW = South China Sea Intermediate Water.

ventilated dense waters sinking to a depth of ~2,500 to 3,000 m during the Heinrich Stadial 1 (HS1) and the Younger Dryas (YD) when the Atlantic meridional overturning circulation weakened (Menviel et al., 2012; Okazaki et al., 2010). However, a few benthic ^{14}C data (Cook & Keigwin, 2015; Galbraith et al., 2007; Lund, 2013) and deep water oxygenation records (Bradtmiller et al., 2010; Galbraith et al., 2007; Jaccard & Galbraith, 2013; Loveley et al., 2017) indicated the absence of direct deep water formation in North Pacific during the HS1 and YD stadials. More data are needed to fully understand the extent to which the intermediate and deep Pacific circulation have changed during the deglacial period. In the western Pacific, a series of marginal basins are connected to the open ocean through a few narrow passages. Due to the depth difference of these passages, each marginal basin could only exchange specific water masses with the open Pacific Ocean. Paleo-oxygenation records from these marginal basins provide new evidence on the intermediate and deep circulation in the western Pacific.

The South China Sea (SCS) is the largest semienclosed marginal sea with the Luzon Strait connecting to the west Pacific. Deep waters below ~1,500 m in the SCS are sourced by the PDW through the Luzon Strait with the sill depth of ~2,400 m (Figure 1a). The SCS Deep Water (SCSDW) is oxygen rich and well ventilated at present (Wang et al., 2018). The SCSDW upwells in southern SCS and forms intermediate waters at depths of 400–1,500 m (termed the *South China Sea Intermediate Water*; SCSIW), which have the lowest oxygen concentration (Li & Qu, 2006) (Figure 1b). The Okinawa Trough (OT) is a back-arc basin in the northwest Pacific that links to the open Pacific through the Kerama Gap, where the greatest depth is 1,050 m. At present, bottom waters in the OT are mainly sourced by the low dissolved oxygenated North Pacific Tropical Intermediate Water (Bingham & Lukas, 1995) and the oxygen-rich North Pacific Intermediate Water (NPIW) mainly influences intermediate waters (Figure 1b).

Here we present new benthic foraminiferal $\delta^{13}C$ and redox-sensitive elemental data from a sediment core in the southern SCS that lies within the SCSDW. We place our data with other published data from the deep SCS and OT to provide a broader picture of the past redox history of intermediate and deep waters in the western Pacific. Our data do not appear to support the hypothesis that the strengthened NPIW intruded into the deep SCS below 1,600 m during the LGM and subsequent deglacial period.

2. Materials and Methods

Sediment core HYIV2015-B9 (hereafter B9; 10.2484°N, 112.7325°E; 2,603 m water depth) was retrieved during the cruise HYIV20150816 of R/V Haiyang IV in 2015 (Figure 1) from the northern slope of Nansha Terrace in the southern SCS. The upper section of core B9 (165 cm; total length: 455 cm) was analyzed in this study. Samples were taken at 1- to 4- and 2- to 4-cm intervals for geochemical analyses and stable oxygen and carbon isotopic measurements, respectively. Epifaunal benthic foraminifera *Cibicidoides wuellerstorfi* were picked from the >250-μm-size fractions for isotopic analysis. The $\delta^{13}C$ and $\delta^{18}O$ were measured on a Thermo Scientific MAT 253 mass spectrometer and calibrated to the PDB standard. For the elemental analysis, approximately 2-g freeze-dried sediments were crushed into powder. Major and trace element abundances were determined using ICP-OES (IRIS Intrepid II XSP) and ICP-MS (Perkin-Elmer Elan 9000). The measurement methodology of Qi et al. (2000) was followed. The accuracy of this analytical method, determined by analyzing standard reference materials (Chinese marine sediments: GBW 07315 and GBW 07316) and BHVO-2 (U.S. Geological Survey-basalt), is better than 3%.

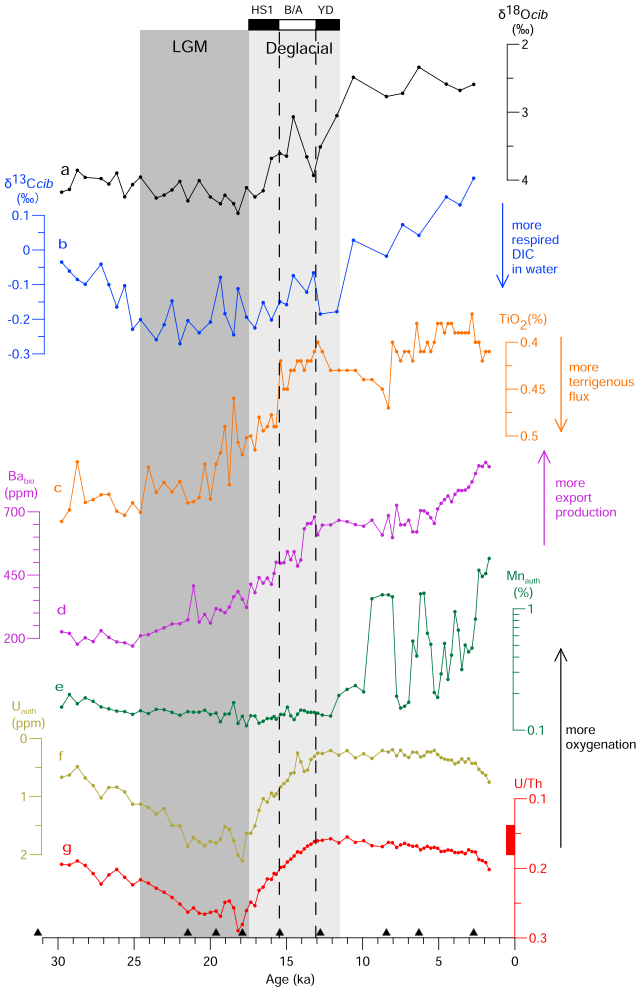

Figure 2. Paleo-proxy records of core B9 showing variations in dissolved inorganic carbon (DIC) $\delta^{13}C$, benthic redox condition, and marine productivity during the last 30 ka. (a) and (b) $\delta^{18}O$ and $\delta^{13}C$ on *C. wuellerstorfi*, (c) TiO_2, (d) biogenic Ba, (e) authigenic Mn, (f) authigenic U, and (g) U/Th. The U/Th range of terrigenous sediment from the ODP site 1143 (Wan et al., 2017) is marked by a red bar on the *y*-axis (g). The Last Glacial Maximum (LGM) and the deglacial period, including the Heinrich Stadial 1 (HS1), Younger Dryas (YD), and Bølling/Allerød Interstadial (B/A) are highlighted by gray vertical bars and dashed lines.

The stratigraphy of upper 165 cm of core B9 is constrained by nine ^{14}C-accelerator mass spectrometric (^{14}C-AMS) dates (Table S1 in the supporting information). Seven ^{14}C-AMS dates were measured on planktonic foraminifer *Globigerinoides sacculifer* and the other two dates were obtained on mixed *G. sacculifer* and *G. ruber* foraminifers. All ^{14}C-AMS dates were calibrated to the calendar year before present using the online calibration program CALIB 7.0.4 (Stuiver et al., 2018) and no additional regional reservoir age was used (Kienast et al., 2001). Sedimentation rates vary between 2 and 8 cm/kyr at the site of B9 (Figure S1).

It has been known that Titanium (Ti) in marine sediments is mainly derived from terrigenous sources (Goldberg & Arrhenius, 1958; Wei et al., 2003). Hence, the abundance of the terrigenous component in marine sediments can be estimated from Ti concentrations. Authigenic or biogenic concentrations of the elements barium (Ba), phosphorus (P), manganese (Mn), nickel (Ni), chromium (Cr), vanadium (V), and uranium (U) at site B9 are estimated by subtracting the terrigenous contribution from bulk-sediment elemental concentrations by using the formula (1). Average elemental concentrations of detrital components of core NS90-103 (Wei et al., 2000) and the Ocean Drilling Program (ODP) site 1143 (Wan et al., 2017) (Figure 1a) are taken to represent the composition of terrigenous sediments in this study area.

$$M_{auth} \text{ or } M_{bio} = M_{bulk} - Ti_{bulk} \times M_{detr}/Ti_{detr} \quad (1)$$

where M_{auth} and M_{bio} are the elemental concentrations of authigenic or biogenic components, M_{bulk} is the elemental concentration of bulk sediments, and M_{detr}/Ti_{detr} is the element ratio relative to Ti of terrigenous sediments assessed from core NS90-103 (Wei et al., 2000) and the ODP site 1143 (Wan et al., 2017).

3. Results

Benthic foraminiferal $\delta^{18}O$ of B9 decreases from 4.21‰ to 2.75‰ with a gradual change from the LGM to Holocene (Figure 2a). The *C. wuellerstorfi* $\delta^{13}C$ displays the minimum value (about −0.20‰) during the LGM which is about 0.29‰ lower than those of the Holocene, consistent with the $\delta^{13}C$ stack of the PDW (Lisiecki, 2010). During the deglacial period, the $\delta^{13}C$ shows a slowly rising trend with two negative excursions that might correspond to the cold stadials (HS1 and YD; Figure 2b).

The concentrations of K, Al, Rb, Ti, and Zr from B9 show similar patterns of variation (Figure 2c) with the highest values during the last glaciation. The rapid decrease in terrestrial elemental concentrations started at ~19.5 ka and terminated at 13 ka. Most of the terrestrial elemental concentrations have slightly increased until the middle Holocene. Four elements, namely, Ba, P, Sr, and Ca, show similar variations in concentrations with the lowest values between 30 and 25 ka. The biogenic Ba shows a slow increase from the LGM to the HS1 and a rapid increase during the Bølling/Allerød (B/A) interstadial (Figure 2d). The concentrations of authigenic Mn and Ni vary similarly, showing the highest values during the Holocene (Figures 2e and S3e). The Mn/Ti during the Holocene (3.12 on average) is remarkably higher than the ratio of terrigenous sediments in the southwest SCS (0.12 at NS90-103, Wei et al., 2000, and 0.22 at the ODP site 1143, Wan et al., 2017). The Mn_{auth} is five times higher during the Holocene compared to the last glaciation. The rapid increase in Mn_{auth} is identified at 10 ka. The variations of authigenic U and V are opposite to the Mn_{auth}, showing enrichment during the LGM (Figures 2f and S3f). The most U-enriched sediment was dated between 22 and 17.5 ka. Moreover, the bulk U/Ti of the LGM sediments at B9 (11.2×10^{-4} on average) is higher than that of terrigenous sediments ($5.0–6.0 \times 10^{-4}$) at NS90-103 (Wei et al., 2000) and the ODP site 1143 (Wan et al., 2017).

4. Discussion

4.1. The Redox History of the Southern SCS Since the LGM

In marine environments, oxic bottom waters often promote the authigenic enrichment of Mn in an insoluble oxyhydroxide or oxide; however, U and V accumulate in marine sediments under suboxic conditions (Calvert & Pedersen, 1993). The Ni reacts similar to Mn in seawater and sediments, that is, it can be scavenged by the Mn oxides in the oxidizing environment (Santos-Echeandia et al., 2009). In the southern SCS, the Mn enrichment in sea-bottom sediments mainly occurs within SCSDW with high dissolved O_2 concentrations at present (Figure S2). The significant Mn enrichment in the upper 30 cm at B9 indicates a well-oxidizing environment during the Holocene (Figure 2e). The obvious enrichment of U and V of the LGM sediments suggests a less oxidizing environment during this period (Figures 2f and S3f). Two redox indices, namely, U/Th and V/Cr which show the highest values during the LGM, lend further support to the inference by authigenic elemental concentrations (Figures 2g and S3 g). The influence of sediment provenance variations cannot be completely excluded. However, the changes in redox proxies (Mn/Ti, U/Ti, U/Th, and V/Cr) from the LGM to the Holocene at B9 are strikingly larger than the glacial/interglacial variations in these ratios of terrigenous sediments in southern SCS (Wan et al., 2017; Wei et al., 2000), suggesting that the oscillation of redox conditions plays a dominant role. In summary, redox-sensitive elemental data of core B9 suggest that the change in oxygenation features of sea bottom sediments at 2,603 m in southern SCS started at 18 ka and the oxygenation has been set to the modern condition since the YD.

4.2. The Decoupling Between Productivity and Oxygenation of Sea-Bottom Sediments

The redox state of sediments is controlled by the diagenetic respiration of labile organic matter together with the bottom water oxygenation. The U enrichment and Mn depletion in the LGM sediments at B9 likely resulted from the greater export of organic matter to the seafloor due to higher marine productivity. Biogenic Ca and Sr data at the site B9 and a nearby core NS93-5 suggest the higher production of calcareous plankton in southern SCS during the Holocene (Wei et al., 2003). Most of published opal records such as NS93-5 (Chen et al., 2008), GIK17957 (Jian et al., 2000), ODP site 1143 (Wang & Li, 2003) and MD97-2142 (Shiau et al., 2008) are consistent with our biogenic Ba and P data (Figure 2d). Foraminiferal and radiolarian-based studies suggest that the higher surface-water productivity during the interglacial period in southern SCS was likely due to upwelling resulted from the strengthening of summer monsoon (Jian et al., 2001; Wang & Abelmann, 2002). The U/Th and V/Cr of B9 (this study) and NS93–5 (Wei et al., 2003) suggest the absence of sulfate reduction in the deep SCS even during the LGM (Jones & Manning, 1994). In the absence of sulfate reduction, the biogenic Ba concentration has not been significantly modified by suboxic diagenesis and the initial concentration has been recorded when buried. Our authigenic Mn, U, and Ba data appear to contradict the hypothesis that the redox variation of sea-bottom sediments in southern deep SCS is mainly associated with the productivity inferred by organic proxies (Li et al., 2017). Therefore, we hypothesize that the U_{auth} could be a proxy for past changes in bottom-water oxygenation due to the lack of positive correlation with biogenic Ba concentrations at B9. However, the influence from the enhanced bottom-water oxygen consumption upstream of this site cannot be entirely excluded as the export productivity was higher in northern SCS due to the intense winter monsoon during the last glacial period (Jian et al., 2001; Wang et al., 2007).

4.3. The Oxygenation History of the SCSDW

Three core sites (MD97-2142, NS93-5, and B9; Figure 1) within the southern SCSDW consistently record a marked increase in the oxygenation from the last glaciation to the Holocene (Figures 3b, 3c, and 3f). According to authigenic U records from NS93-5 at 1,792 m and B9 at 2,603 m, the increase in oxygenation started at 18 ka, that is, at the onset of the last glacial termination (Figures 3c and 3f). The synchronous change in oxygenation of entire deep waters cannot be simply explained by the shift of the low-oxygen SCSIW (Löwemark et al., 2009). In the SCS, the bathymetric profile of *C. wuellerstorfi* $\delta^{13}C$ from the late Holocene has a similar trend with the distribution of $\delta^{13}C$ of seawater $\sum CO_2$ (Lin, 2003; Wan et al., 2018). It generally supports the point that the *C. wuellerstorfi* $\delta^{13}C$ serves as a reliable proxy for dissolved inorganic carbon (DIC) $^{13}C/^{12}C$ (Duplessy et al., 1988). Recently compiled benthic foraminiferal $\delta^{13}C$ profiles in the SCS by Wan et al. (2018) show similar hydrographic structures between the LGM and late Holocene and a small vertical expansion of intermediate waters during the last glacial period. The *C. wuellerstorfi* $\delta^{13}C$

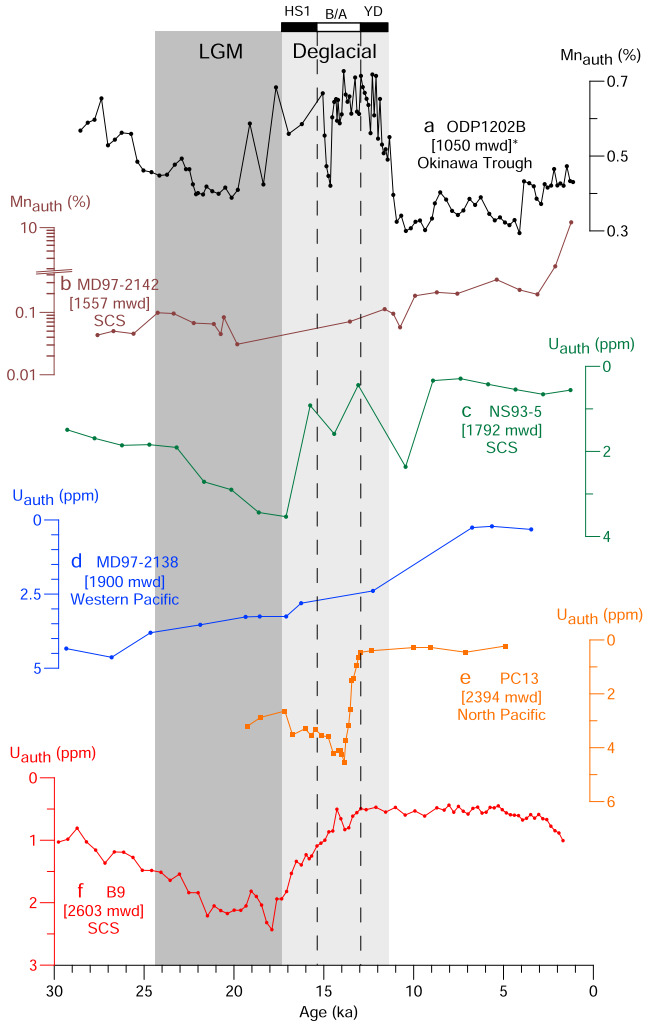

Figure 3. Comparison of authigenic Mn and U records in South China Sea, Okinawa Trough, and open Pacific. (a) ODP site 1202B (Dou et al., 2015), (b) MD97-2142 (Löwemark et al., 2009), (c) NS93-5 (Wei et al., 2003), (d) MD97-2138 (Bradtmiller et al., 2010), (e) PC13 (Jaccard & Galbraith, 2013), and (f) B9 (this study). Cores within the SCSDW and PDW from 1,557 to 2,603 m show an obvious enrichment in Mn and depletion in U during the Holocene compared to the LGM. However, the ODP site 1202B in the Okinawa Trough has a significant accumulation of Mn_{auth} during the deglacial period and the lowest Mn_{auth} during the Holocene. *The depth shown is that of the Kerama. Location of cores is shown in Figure 1.

records from multiple cores in southern SCS also indicate minor changes in the intermediate and deep water circulation since the last glaciation (Figure S4). The more negative $\delta^{13}C$ of core MD97-2151 near the boundary between the SCSIW and the SCSDW (at about 1,500 m) demonstrates that the SCSIW has been more depleted in $\delta^{13}C$ relative to the SCSDW during the last 30 ka. The absence of pronounced variations in Mn concentrations at site GIK17925 might be due to the predominance of terrigenous components in the northeast deep SCS because the Mn/Ti fluctuates around the value for post-Archean Australian shale (PAAS; Taylor and McLennan (1985)). In contrast to GIK17925, the Mn/Ti in the southern deep SCS (e.g., B9, NS93-5) is much higher than the PAAS value, suggesting lower terrestrial dominance. In summary, the combined U_{auth} and benthic $\delta^{13}C$ data in the southern SCS indicate that the U_{auth} decrease from the LGM to the Holocene present in waters deeper than 1,600 m can be reasonably explained by the increase in oxygen concentrations in the SCSDW.

4.4. The Oxygenation History Between the SCS and OT/Open Pacific Ocean

In the southern OT, ODP site 1202B recorded the highest authigenic Mn and positive Ce anomaly during the deglacial period (Dou et al., 2015). Two authigenic Mn peaks could be correlated to the cold stadials (HS1 and YD); however, due to inadequate age constraint, the correlation between the Mn peaks and cold stadials is tenuous (Figure 3a). In any event, the redox record at ODP site 1202B is consistent with the benthic $\delta^{13}C$ record of core GH08-2004 at 1,166 m near the OT (Kubota et al., 2015), suggesting an increase in bottom water oxygenation in the OT during the HS1 and YD stadials (Figure 4).

Deep waters in two marginal basins, that is, the SCS and the OT, exhibit different oxygenation history since the last glaciation. The same comparison was equally applicable to numerous published records that deal with the Pacific intermediate and deep waters (Jaccard & Galbraith, 2012, 2013; Kim et al., 2017). The high oxygen concentrations reflected by redox-sensitive elements (Crusius et al., 2004; Jaccard & Galbraith, 2013; Kim et al., 2017), foraminiferal assemblages (Kim et al., 2017) and benthic foraminiferal $\delta^{13}C$ (Lembke-Jene et al., 2017; Max et al., 2014) were reported from intermediate waters (mostly shallower than 1,500 m) in northern Pacific during the deglacial cold stadials. The increase in oxygenation was possibly associated with the stronger intermediate waters ventilation due to deepening and strengthening of the NPIW (Ahagon et al., 2003; Max et al., 2014). However, most U_{auth} records in deep Pacific Ocean show the highest concentrations during the LGM and minima during the Holocene (Bradtmiller et al., 2010;Galbraith et al., 2007 ; Jaccard & Galbraith, 2012, 2013; Loveley et al., 2017) (Figures 3d and 3e). Authigenic U concentrations in conjunction with contemporaneous biogenic opal flux data could be only ascribed to the increase in deep water oxygen concentrations from the last glaciation to the Holocene (Bradtmiller et al., 2010; Galbraith et al., 2007; Loveley et al., 2017). The increase in oxygenation of the PDW is consistent with the decrease in ventilation ages which were widely reported for the open Pacific Ocean (De La Fuente et al., 2015; Galbraith et al., 2007; Skinner et al., 2010). After the Bølling/Allerød interstadial, the oxygenation of SCSDW at site B9 rose to the level of the Holocene, consistent with most U_{auth} records in the northern and eastern Pacific (Galbraith et al., 2007; Jaccard & Galbraith, 2012, 2013; Loveley et al., 2017) and the Southern Ocean (Jaccard et al., 2016). In addition, the decrease in U_{auth} at B9 in the southern SCS also preceded the opening of southwestern gateways to the Indian Ocean (Voris, 2000) suggesting that the increase in deep water oxygenation was not mainly

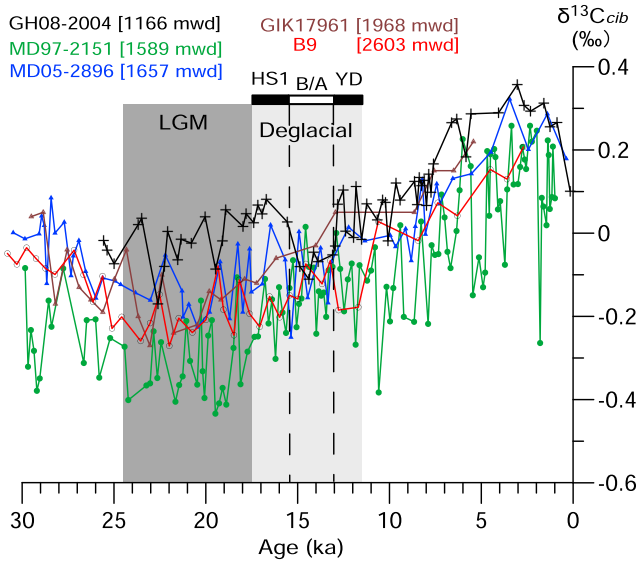

Figure 4. Carbon stable isotope records of *C. wuellerstorfi* from cores GH08-2004 (Kubota et al., 2015), GIK17961 (Wang et al., 1999), MD97-2151 (Wei et al., 2006), MD05-2896 (Wan & Jian, 2014), and B9 (this study) in the southern South China Sea and the adjacent Okinawa Trough. The core MD97-2151 was raised near the lower boundary of the SCSIW. Cores MD05-2896, GIK 17961, and B9 were retrieved within the SCSDW. Location of cores is shown in Figure 1.

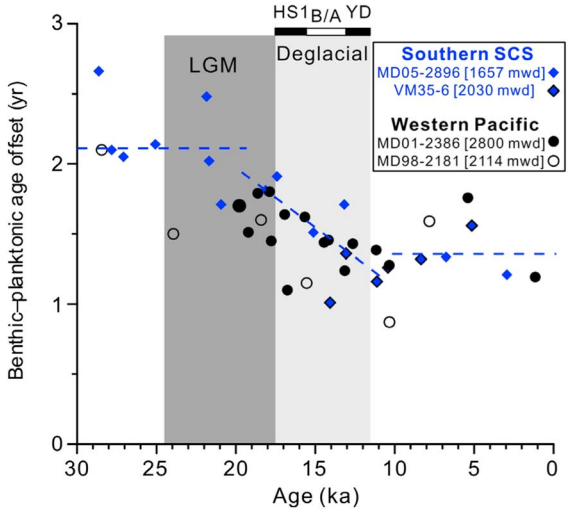

Figure 5. Comparison of benthic-planktonic ^{14}C age offset in the southern South China Sea and western tropical Pacific. Dashed lines mark the variation trend of B-P ^{14}C ages in the southern SCS, which is similar to the B-P ages of the PDW in the western Pacific. MD05-2896 (Wan & Jian, 2014); VM35-6 (Andree et al., 1986); MD01-2386 (Broecker et al., 2008); MD98-2181 (Stott et al., 2007). Location of cores is shown in Figure 1.

influenced by the sea-level change. If our records at B9 are compared with the intermediate and deep water oxygenation history in open Pacific and OT, it is clearly apparent that the variation in oxygenation of the SCSDW has been in phase with the Southern Ocean-sourced PDW since the last glaciation.

The inference on the source of the SCSDW based on redox-sensitive elements in the study is supported by recent circulation records from ventilation ages (Wan & Jian, 2014), benthic foraminiferal $\delta^{13}C$ (Wan et al., 2018) and deep water ε_{Nd} (Wu et al., 2015) in the SCS. The ^{14}C age difference between planktonic and benthic foraminifers (B-P) from sediment cores in southern deep SCS (MD05–2896 and VM 35–6) mostly falls within the range of the age-difference from two western Tropic Pacific records (MD98-2181 and MD01-2386) at 2,100–2,800 m water depths (Broecker et al., 2008; Stott et al., 2007) (Figure 5). Broecker et al. (2004) dated terrestrial wood from the glacial deposits and found no large change in surface reservoir ages (R) in the open western Pacific during the glacial period. Kienast et al. (2001) used a constant (400 years) reservoir to construct an age model for alkenone SST records in southern SCS. The authors found that the Bølling warming in the southern SCS was synchronous with the Greenland Ice Sheet Project 2 ice core, suggesting that the surface R during the deglaciation was similar to the present. Therefore, the B-P ages in the southern deep SCS and the western tropical Pacific mainly reflect the true change in the PDW ventilation. The recently compiled *C. wuellerstorfi* $\delta^{13}C$ profiles also support no changes in deep water sources in the SCS during the LGM, with the evidence of a decreasing $\delta^{13}C$ trend from the Southern Ocean to the SCS and sub-Arctic Pacific (Wan et al., 2018; this study). The SCSDW circulation records in deep SCS (Andree et al., 1986; Wan & Jian, 2014; Wan et al., 2018; Wu et al., 2015; this study) match with its oxygenation from redox-sensitive elemental data in this study. During the LGM, the poorly ventilated PDW intruded into the deep SCS and conditioned the accumulation of authigenic U in sea-bottom sediments. The increase in deep water oxygenation in the deep SCS and the western Pacific Ocean from the LGM to Holocene was associated with the increased ventilation rate of the PDW.

5. Summary

A sediment core from the southern SCS is used to reconstruct the deep water oxygenation history. Our records are placed with published records from other marginal basins and the open Pacific Ocean. These records provide strong evidence for the variations in water-mass structures in the western Pacific Ocean since the LGM, showing the deepening of the NPIW during the deglacial cold stadials. It is apparent that the NPIW would have filled the deep OT during the HS1 and YD stadials but it would not have influenced waters deeper than 1,600 m in the SCS. The SCSDW would have been from the Southern Ocean-sourced PDW since the LGM, and the oxygenation variation seems to be determined by the change in the ventilation rates of its source waters. The oxygenation records from intermediate and deep waters in the western Pacific Ocean seem to agree with the general circulation model results (Chikamoto et al., 2012) and most paleo-proxy data (Bradtmiller et al., 2010; Jaccard & Galbraith, 2012; Loveley et al., 2017; Moffitt et al., 2015) in the Pacific. These data suggest a strengthened intermediate-depth meridional overturning in the Pacific Ocean in response to a weakening of the Atlantic meridional overturning circulation during cold stadials of the last deglacial period.

Acknowledgments

We would like to thank all crew of the R/V Haiyang IV of Guangzhou Marine Geological Survey of the 2015 cruise. We acknowledge L. Löwemark for sharing elemental data of cores MD97-2142 and GIK 17925. The manuscript is greatly improved by comments from two anonymous reviewers and by Editor T. Ilyina. David J. W. Piper is thanked for reviewing the final version of this paper. Our work is supported by the National Natural Science Foundation of China (41676031, 41306047, 41676056, 91428205, and 41776064), the Strategic Priority Research Program of the Chinese Academy of Sciences (XDA11030103 and XDA13010102), the Guangdong Natural Science Foundation (2017A030313252), and the Youth Innovation Promotion Association of CAS (2017395). The data presented in this paper are listed in the supporting information.

References

Ahagon, N., Ohkushi, K., Uchida, M., & Mishima, T. (2003). Mid-depth circulation in the Northwest Pacific during the last deglaciation: Evidence from foraminiferal radiocarbon ages. *Geophysical Research Letters*, *30*(21), 2097. https://doi.org/10.1029/2003GL018287

Andree, M., Oeschger, H., Broecker, W., Beavan, N., Klas, M., Mix, A., et al. (1986). Limits on the ventilation rate for the Deep Ocean over the last 12000 years. *Climate Dynamics*, *1*(1), 53–62. https://doi.org/10.1007/bf01277046

Bingham, F. M., & Lukas, R. (1995). The distribution of intermediate water in the western equatorial Pacific during January–February 1986. *Deep Sea Research Part I*, *42*(9), 1545–1573. https://doi.org/10.1016/0967-0637(95)00064-D

Bradtmiller, L. I., Anderson, R. F., Sachs, J. P., & Fleisher, M. Q. (2010). A deeper respired carbon pool in the glacial equatorial Pacific Ocean. *Earth and Planetary Science Letters*, *299*(3–4), 417–425. https://doi.org/10.1016/j.epsl.2010.09.022

Broecker, W. S., Barker, S., Clark, E., Hajdas, I., Bonani, G., & Stott, L. (2004). Ventilation of the glacial deep Pacific Ocean. *Science*, *306*(5699), 1169–1172. https://doi.org/10.1126/science.1102293

Broecker, W. S., Clark, E., & Barker, S. (2008). Near constancy of the Pacific Ocean surface to mid-depth radiocarbon-age difference over the last 20 kyr. *Earth and Planetary Science Letters*, *274*(3-4), 322–326. https://doi.org/10.1016/j.epsl.2008.07.035

Calvert, S. E., & Pedersen, T. F. (1993). Geochemistry of recent oxic and anoxic marine sediments: Implications for the geological record. *Marine Geology*, *113*(1-2), 67–88. https://doi.org/10.1016/0025-3227(93)90150-T

Chen, M. H., Li, Q. Y., Zhang, L. L., Zheng, F., Lu, J., Xiang, R., et al. (2008). Systematic biotic responses to palaeoenvironmental change in the Late Pleistocene southern South China Sea: A preliminary study. *Journal of Quaternary Science*, *23*(8), 803–815. https://doi.org/10.1002/jqs.1178

Chikamoto, M. O., Menviel, L., Abe-Ouchi, A., Ohgaito, R., Timmermann, A., Okazaki, Y., et al. (2012). Variability in North Pacific intermediate and deep water ventilation during Heinrich events in two coupled climate models. *Deep Sea Research, Part II*, *61-64*, 114–126. https://doi.org/10.1016/j.dsr2.2011.12.002

Cook, M. S., & Keigwin, L. D. (2015). Radiocarbon profiles of the NW Pacific from the LGM and deglaciation: Evaluating ventilation metrics and the effect of uncertain surface reservoir ages. *Paleoceanography*, *30*, 174–195. https://doi.org/10.1002/2014PA002649

Costa, K. M., Anderson, R. F., McManus, J. F., Winckler, G., Middleton, J. L., & Langmuir, C. H. (2018). Trace element (Mn, Zn, Ni, V) and authigenic uranium (aU) geochemistry reveal sedimentary redox history on the Juan de Fuca ridge, North Pacific Ocean. *Geochimica et Cosmochimica Acta*, *236*, 79–98. https://doi.org/10.1016/j.gca.2018.02.016

Crusius, J., Pedersen, T. F., Kienast, S., Keigwin, L., & Labeyrie, L. (2004). Influence of Northwest Pacific productivity on North Pacific Intermediate Water oxygen concentrations during the Bølling-Allerød interval (14.7–12.9 ka). *Geology*, *32*(7), 633–636. https://doi.org/10.1130/g20508.1

De La Fuente, M., Skinner, L., Calvo, E., Pelejero, C., & Cacho, I. (2015). Increased reservoir ages and poorly ventilated deep waters inferred in the glacial eastern equatorial Pacific. *Nature Communications*, *6*(1), 7420–7411. https://doi.org/10.1038/ncomms8420

Dou, Y. G., Yang, S. Y., Li, C., Liu, J. H., & Bi, L. (2015). Deepwater redox changes in the southern Okinawa trough since the last glacial maximum. *Progress in Oceanography*, *135*, 77–90. https://doi.org/10.1016/j.pocean.2015.04.007

Duplessy, J. C., Shackleton, N. J., Fairbanks, R. G., Labeyrie, L., Oppo, D., & Kallel, N. (1988). Deepwater source variations during the last climatic cycle and their impact on the global Deepwater circulation. *Paleoceanography*, *3*(3), 343–360. https://doi.org/10.1029/PA003i003p00343

Galbraith, E. D., Jaccard, S. L., Pedersen, T. F., Sigman, D. M., Haug, G. H., Cook, M., et al. (2007). Carbon dioxide release from the North Pacific abyss during the last deglaciation. *Nature*, *449*(7164), 890–893. https://doi.org/10.1038/nature06227

Garcia, H. E., Locarnini, R. A., Boyer, T. P., Antonov, J. I., Baranova, O. K., Zweng, M. M., et al. (2014). In S. Levitus, & A. Mishonov (Eds.), *World Ocean Atlas 2013, Volume 3: Dissolved Oxygen, Apparent Oxygen Utilization, and Oxygen Saturation* (Vol. 75, pp. 1–27). Silver Spring, MD: NOAA Atlas NESDIS.

Goldberg, E. D., & Arrhenius, G. O. S. (1958). Chemistry of Pacific pelagic sediments. *Geochimica et Cosmochimica Acta*, *13*(2-3), 153–212. https://doi.org/10.1016/0016-7037(58)90046-2

Jaccard, S. L., & Galbraith, E. D. (2012). Large climate-driven changes of oceanic oxygen concentrations during the last deglaciation. *Nature Geoscience*, *5*(2), 151–156. https://doi.org/10.1038/ngeo1352

Jaccard, S. L., & Galbraith, E. D. (2013). Direct ventilation of the North Pacific did not reach the deep ocean during the last deglaciation. *Geophysical Research Letters*, *40*, 199–203. https://doi.org/10.1029/2012GL054118

Jaccard, S. L., Galbraith, E. D., Martínez-García, A., & Anderson, R. F. (2016). Covariation of deep Southern Ocean oxygenation and atmospheric CO_2 through the last ice age. *Nature*, *530*(7589), 207–210. https://doi.org/10.1038/nature16514

Jian, Z. M., Huang, B. Q., Kuhnt, W., & Lin, H. L. (2001). Late Quaternary upwelling intensity and east Asian monsoon forcing in the South China Sea. *Quaternary Research*, *55*(03), 363–370. https://doi.org/10.1006/qres.2001.2231

Jian, Z. M., Wang, P. X., Chen, M. P., Li, B., Zhao, Q., Buhring, C., et al. (2000). Foraminiferal responses to major Pleistocene paleoceanographic changes on the southern South China Sea. *Paleoceanography*, *15*(2), 229–243. https://doi.org/10.1029/1999PA000431

Jones, B., & Manning, D. A. C. (1994). Comparison of geochemical indices used for the interpretation of palaeoredox conditions in ancient mudstones. *Chemical Geology*, *111*(1-4), 111–129. https://doi.org/10.1016/0009-2541(94)90085-X

Kienast, M., Steinke, S., Stattegger, K., & Calvert, S. E. (2001). Synchronous tropical South China Sea SST change and Greenland warming during deglaciation. *Science*, *291*(5511), 2132–2134. https://doi.org/10.1126/science.1057131

Kim, S., Khim, B. K., Ikehara, K., Itaki, T., Shibahara, A., & Yamamoto, M. (2017). Millennial-scale changes of surface and bottom water conditions in the northwestern Pacific during the last deglaciation. *Global and Planetary Change*, *154*, 33–43. https://doi.org/10.1016/j.gloplacha.2017.04.009

Köhler, P., Fischer, H., Munhoven, G., & Zeebe, R. E. (2005). Quantitative interpretation of atmospheric carbon records over the last glacial termination. *Global Biogeochemical Cycles*, *19*, GB4020. https://doi.org/10.1029/2004GB002345

Kubota, Y., Kimoto, K., Itaki, T., Yokoyama, Y., Miyairi, Y., & Matsuzaki, H. (2015). Bottom water variability in the subtropical northwestern Pacific from 26 kyr BP to present based on mg/ca and stable carbon and oxygen isotopes of benthic foraminifera. *Climate of the Past*, *11*(6), 803–824. https://doi.org/10.5194/cp-11-803-2015

Lembke-Jene, L., Tiedemann, R., Nürnberg, D., Kokfelt, U., Kozdon, R., Max, L., et al. (2017). Deglacial variability in Okhotsk Sea intermediate water ventilation and biogeochemistry: Implications for North Pacific nutrient supply and productivity. *Quaternary Science Reviews*, *160*, 116–137. https://doi.org/10.1016/j.quascirev.2017.01.016

Li, D. W., Chiang, T. L., Kao, S. J., Hsin, Y. C., Zheng, L. W., Yang, J. Y., et al. (2017). Circulation and oxygenation of the glacial South China Sea. *Journal of Asian Earth Sciences*, *138*, 387–398. https://doi.org/10.1016/j.jseaes.2017.02.017

Li, L., & Qu, T. D. (2006). Thermohaline circulation in the deep South China Sea basin inferred from oxygen distributions. *Journal of Geophysical Research*, *111*, C05017. https://doi.org/10.1029/2005JC003164

Lin, H. L. (2003). Late Quaternary deep-water circulation in the South China Sea. *Terrestrial, Atmospheric and Oceanic Sciences*, *14*(3), 321–333. https://doi.org/10.3319/TAO.2003.14.3.321(O)

Lisiecki, L. E. (2010). A simple mixing explanation for late Pleistocene changes in the Pacific-South Atlantic benthic $\delta^{13}C$ gradient. *Climate of the Past*, *6*(3), 305–314. https://doi.org/10.5194/cp-6-305-2010

Loveley, M. R., Marcantonio, F., Wisler, M. M., Hertzberg, J. E., Schmidt, M. W., & Lyle, M. (2017). Millennial-scale iron fertilization of the eastern equatorial Pacific over the past 100,000 years. *Nature Geoscience*, *10*(10), 760–764. https://doi.org/10.1038/ngeo3024

Löwemark, L., Steinke, S., Wang, C. H., Chen, M. T., Müller, A., Shiau, L. J., et al. (2009). New evidence for a glacioeustatic influence on deep water circulation, bottom water ventilation and primary productivity in the South China Sea. *Dynamics of Atmospheres and Oceans*, *47*(1–3), 138–153. https://doi.org/10.1016/j.dynatmoce.2008.08.004

Lund, D. C. (2013). Deep Pacific ventilation ages during the last deglaciation: Evaluating the influence of diffusive mixing and source region reservoir age. *Earth and Planetary Science Letters*, *381*, 52–62. https://doi.org/10.1016/j.epsl.2013.08.032

Max, L., Lembke-Jene, L., Riethdorf, J. R., Tiedemann, R., Nürnberg, D., Kühn, H., & Mackensen, A. (2014). Pulses of enhanced North Pacific Intermediate Water ventilation from the Okhotsk Sea and Bering Sea during the last deglaciation. *Climate of the Past*, *9*(6), 6221–6253. https://doi.org/10.5194/cpd-9-6221-2013

Menviel, L., Timmermann, A., Elison Timm, O., Mouchet, A., Abe-Ouchi, A., Chikamoto, M. O., et al. (2012). Removing the North Pacific halocline: Effects on global climate, ocean circulation and the carbon cycle. *Deep Sea Research Part II*, *61-64*, 106–113. https://doi.org/10.1016/j.dsr2.2011.03.005

Mikolajewicz, U., Crowley, T. J., Schiller, A., & Voss, R. (1997). Modelling teleconnections between the North Atlantic and North Pacific during the younger Dryas. *Nature*, *387*(6631), 384–387. https://doi.org/10.1038/387384a0

Moffitt, S. E., Hill, T. M., Roopnarine, P. D., & Kennett, J. P. (2015). Response of seafloor ecosystems to abrupt global climate change. *Proceedings of the National Academy of Sciences*, *112*(15), 4684–4689. https://doi.org/10.1073/pnas.1417130112

Monnin, E., Indermühle, A., Dällenbach, A., Flückiger, J., Stauffer, B., Stocker, T. F., et al. (2001). Atmospheric CO_2 concentrations over the last glacial termination. *Science*, *291*(5501), 112–114. https://doi.org/10.1126/science.291.5501.112

Okazaki, Y., Timmermann, A., Menviel, L., Harada, N., Abe-Ouchi, A., Chikamoto, M. O., et al. (2010). Deepwater formation in the North Pacific during the last glacial termination. *Science*, *329*(5988), 200–204. https://doi.org/10.1126/science.1190612

Qi, L., Hu, J., & Gregoire, D. C. (2000). Determination of trace elements in granites by inductively coupled plasma mass spectrometry. *Talanta*, *51*(3), 507–513. https://doi.org/10.1016/S0039-9140(99)00318-5

Rae, J. W., Sarnthein, M., Foster, G. L., Ridgwell, A., Grootes, P. M., & Elliott, T. (2014). Deep water formation in the North Pacific and deglacial CO_2 rise. *Paleoceanography*, *29*, 645–667. https://doi.org/10.1002/2013PA002570

Santos-Echeandia, J., Prego, R., Cobelo-García, A., & Millward, G. E. (2009). Porewater geochemistry in a Galician ria (NW Iberian Peninsula): Implications for benthic fluxes of dissolved trace elements (co, cu, Ni, Pb, V, Zn). *Marine Chemistry*, *117*(1-4), 77–87. https://doi.org/10.1016/j.marchem.2009.05.001

Schlitzer, R. (2002). Interactive analysis and visualization of geoscience data with Ocean Data View. *Computers & Geosciences*, *28*(10), 1211–1218. https://doi.org/10.1016/s0098-3004(02)00040-7

Shiau, L. J., Yu, P. S., Wei, K. Y., Yamamoto, M., Lee, T. Q., Yu, E. F., et al. (2008). Sea surface temperature, productivity, and terrestrial flux variations of the southeastern South China Sea over the past 800000 years (IMAGESMD972142). *Terrestrial, Atmospheric and Oceanic Sciences*, *19*(4), 363–376. https://doi.org/10.3319/TAO.2008.19.4.363(IMAGES

Sigman, D. M., & Boyle, E. A. (2000). Glacial/interglacial variations in atmospheric carbon dioxide. *Nature*, *407*(6806), 859–869. https://doi.org/10.1038/35038000

Skinner, L. C., Fallon, S., Waelbroeck, C., Michel, E., & Barker, S. (2010). Ventilation of the deep Southern Ocean and Deglacial CO_2 rise. *Science*, *328*(5982), 1147–1151. https://doi.org/10.1126/science.1183627

Stott, L., Timmermann, A., & Thunell, R. (2007). Southern hemisphere and Deep-Sea warming led Deglacial atmospheric CO_2 rise and tropical warming. *Science*, *318*(5849), 435–438. https://doi.org/10.1126/science.1143791

Stuiver, M., Reimer, P.J., & Reimer, R.W. (2018). CALIB 7.1 [WWW program] at http://calib.org, accessed 2018-8-11

Talley, L. D. (2013). Closure of the global overturning circulation through the Indian, Pacific, and southern oceans: Schematics and transports. *Oceanography*, *26*(1), 80–97. https://doi.org/10.5670/oceanog.2013.07

Taylor, S. R., & McLennan, S. M. (1985). *The Continental Crust: Its Composition and Evolution*. Oxford: Blackwell Scientific.

Voris, H. K. (2000). Maps of Pleistocene Sea levels in Southeast Asia: Shorelines, river systems and time durations. *Journal of Biogeography*, *27*(5), 1153–1167. https://doi.org/10.1046/j.1365-2699.2000.00489.x

Wan, S., Clift, P., Zhao, D., Hovius, N., Munhoven, G., France-Lanord, C., & Li, T. (2017). Enhanced silicate weathering of tropical shelf sediments exposed during glacial lowstands: A sink for atmospheric CO_2. *Geochimica et Cosmochimica Acta*, *200*, 123–144. https://doi.org/10.1016/j.gca.2016.12.010

Wan, S., Jian, Z., & Dang, H. (2018). Deep hydrography of the South China Sea and deep water circulation in the Pacific since the last glacial maximum. *Geochemistry, Geophysics, Geosystems*, *19*, 1447–1463. https://doi.org/10.1029/2017GC007377

Wan, S., & Jian, Z. M. (2014). Deep water exchanges between the South China Sea and the Pacific since the last glacial period. *Paleoceanography*, *29*, 1162–1178. https://doi.org/10.1002/2013PA002578

Wang, A., Du, Y., Peng, S., Liu, K., & Huang, R. X. (2018). Deepwater characteristics and circulation in the South China Sea. *Deep Sea Research Part I*, *134*, 55–63. https://doi.org/10.1016/j.dsr.2018.02.003

Wang, L. J., Sarnthein, M., Erlenkeuser, H., Grimalt, J., Grootes, P., Heilig, S., et al. (1999). East Asian monsoon climate during the Late Pleistocene: High-resolution sediment records from the South China Sea. *Marine Geology*, *156*(1–4), 245–284. https://doi.org/10.1016/s0025-3227(98)00182-0

Wang, R. J., & Abelmann, A. (2002). Radiolarian responses to paleoceanographic events of the southern South China Sea during the Pleistocene. *Marine Micropaleontology*, *46*(1–2), 25–44. https://doi.org/10.1016/S0377-8398(02)00048-8

Wang, R. J., Jian, Z. M., Xiao, W. S., Tian, J., Li, J. R., Chen, R. H., et al. (2007). Quaternary biogenic opal records in the South China Sea: Linkages to east Asian monsoon, global ice volume and orbital forcing. *Science in China Series D*, *50*(5), 710–724. https://doi.org/10.1007/s11430-007-0041-9

Wang, R. J., & Li, J. (2003). Quaternary high-resolution opal record and its paleoproductivity implication at ODP site 1143, southern South China Sea. *Chinese Science Bulletin*, *48*(4), 363–367. https://doi.org/10.1007/bf03183231

Warren, B. A. (1983). Why is no deep water formed in the North Pacific? *Journal of Marine Research*, *41*(2), 327–347. https://doi.org/10.1357/002224083788520207

Wei, G. J., Gui, X. T., Li, X. H., Chen, Y. W., & Yu, J. S. (2000). Strontium and neodymium isotopic compositions of detrital sediment of NS90-103 from South China Sea: Variations and their paleoclimate implication. *Science in China Series D*, *43*(6), 596–604. https://doi.org/10.1007/BF02879503

Wei, G. J., Huang, C. Y., Wang, C. C., Lee, M. Y., & Wei, K. Y. (2006). High-resolution benthic foraminifer $\delta^{13}C$ records in the South China Sea during the last 150 ka. *Marine Geology*, *232*(3-4), 227–235. https://doi.org/10.1016/j.margeo.2006.08.005

Wei, G. J., Liu, Y., Li, X. H., & Chen, M. H. (2003). High-resolution elemental records from the South China Sea and their paleo-productivity implications. *Paleoceanography*, *18*(2), 1054. https://doi.org/10.1029/2002PA000826

Wu, Q., Colin, C., Liu, Z., Thil, F., Dubois-Dauphin, Q., Frank, N., et al. (2015). Neodymium isotopic composition in foraminifera and authigenic phases of the South China Sea sediments: Implications for the hydrology of the North Pacific Ocean over the past 25 kyr. *Geochemistry, Geophysics, Geosystems*, *16*, 3883–3904. https://doi.org/10.1002/2015GC005871